EPJ Web of Conferences **107**, 02005 (2016)
DOI: 10.1051/epjconf/201610702005

On the properties of $N = 50$ isotones from ^{78}Ni to ^{100}Sn

V. I. Isakov[1,a]

[1] *Petersburg Nuclear Physics Institute, NRC Kurchatov Institute*
188300 Gatchina, Russia

Abstract. By using the self-consistent approach based on the Skyrme functional and with account of pairing correlations, we calculate global properties of nuclei, such as binding energies, one and two-neutron separation energies, density distributions of nucleons, root-mean-square radii of nucleon distributions. For description of excitation energies and transition rates we apply the RPA+BCS approach based on the finite range effective interaction defined by us before. Everywhere, where it is possible, we perform comparison of theoretical results with the experimental data.

Study of evolution of nuclear properties in the long chains of isotopes or isotones, from the extremely proton-excess up to the extremely neutron-excess nuclei is of special theoretical interest, as here one can check the adequacy of the used theoretical models in the broad interval of $(N - Z)/A$. Formerly, [1] we studied in details the chain of the $N = 82$ isotones. Different long chain is represented by the sequence of the nickel isotopes from ^{48}Ni up to ^{78}Ni, where all nuclei, except for ^{78}Ni, turn out to be discovered by the present time. The mentioned chain is of special interest as it includes doubly-magical nucleus ^{48}Ni (which is an extremely proton-excess one), and ^{78}Ni (the last one is strongly neutron-excess, and also the doubly-magical nucleus). This chain also includes doubly magical ^{56}Ni and semi-magical ^{68}Ni. The mentioned series of isotopes was theoretically analyzed by us in [2]. Another long isotopical chain is offered by the succession of tin isotopes having $Z = 50$. The experimental data are available from ^{102}Sn ($N = 52$) up to ^{136}Sn ($N = 86$). These nuclei were theoretically studied by us in [3]. Here, we study chain of isotones from ^{78}Ni up to ^{100}Sn having $N = 50$, this chain includes nuclei ^{88}Sr and ^{90}Zr which also demonstrate some properties of magicity ($Z = 38$ and $Z = 40$, correspondingly).

For description of global properties of nuclei such as their masses, root-mean-square radii of nucleon distributions, one- and two-nucleon separation energies, as well as single-particle energies of protons and neutrons, we apply the Hartree–Fock+BCS method. We also study in the framework of the QRPA approach excitation energies of nuclei and reduced electromagnetic transition rates. To this aim, we use the phenomenological mean field potential that was defined by us before [4]. This potential correctly takes into account isovector terms, which is very important when we consider long isotopic or isotonic chains of nuclei. In our QRPA calculations we also employ effective two-body interaction used by us in our previous papers [2, 3].

To determine nuclear binding energies B in the self-consistent approach, we performed calculations based on the HF+BCS procedure that employs the Skyrme interaction and constant pairing with the corresponding proton and neutron pairing constants G_p and G_n to account for pairing correlations. In this case, one can represent the total energy of an even-even nuclei in its ground state in the following form

$$E = -B = \int H_{\mathrm{HF+BCS}}(\mathbf{r})\, d\mathbf{r} - \frac{\Delta_n^2}{G_n} - \frac{\Delta_p^2}{G_p}. \qquad (1)$$

Here and below, "n" refers to neutrons, while "p" to protons. Pairing correlations in the Hartree–Fock–Bogoliubov energy density $H_{\mathrm{HF+BCS}}(\mathbf{r})$ were considered by introducing the occupancies v_i^2 into the single-particle density of matter, as well as into the kinetic energy and spin densities. In this way, the Hartree–Fock problem with modified densities was solved in coordinate representation, while the iteration procedure was applied for joint solution of the HF+BCS equations. In cases of odd, or odd–odd nuclei one should add to (1) the quasiparticle energy (energies) E_{j_0} of an odd particle (particles),

$$E_{j_{0,p},j_{0,n}} = \sqrt{(\varepsilon_{j_{0,p},j_{0,n}} - \lambda_{p,n})^2 + \Delta_{p,n}^2}\,.$$

In our self-consistent calculations we used parameters of the Skyrme 3 interaction, while the pairing constants G were close to those from [5]. The exchange Coulomb terms were treated in the Slater approximation. In our calculations of binding and single-particle energies as well as of the quasiparticle characteristics, we considered all bounded and quasistationary single-particle levels.

One can see the values of the obtained binding energies for even isotones having $N = 50$ in Fig. 1. In accordance

[a] e-mail: visakov@thd.pnpi.spb.ru

with the experiment, the maximal binding energy per one nucleon happens for isotones having $A \sim 90(88)$.

In Fig. 2, we show both theoretical and empirical values of the two-proton separation energies S_{2p} for the sequence of even isotones having $N = 50$, where calculations were performed in the framework of the HF+BCS method. One can see a good agreement with the experiment. The comparison of theoretical (HF+BCS method) and empirical values of the one-proton separation energies S_p for the chains of isotones having $N = 50$ and even and odd values of Z is shown in Fig. 3. Analogous calculations, but in the framework of phenomenological (WS+BCS) scheme were performed by using the ansatz: $S_p(nlj)(Z+1,N) = -\lambda_p(Z) - E^{min}_{nlj}(Z+1)$ and $S_p(nlj)(Z,N) = -\lambda_p(Z) + E^{min}_{nlj}(Z-1)$; Z and N are even.

In our phenomenological calculations we used the mean-field potential of the form

$$V(\mathbf{r},\sigma) = U\cdot f(r) + U_{ls}\cdot\frac{1}{r}\frac{df}{dr}\,\mathbf{l}\cdot\mathbf{s}\,;\;\; f(r) = \frac{1}{1+\exp((r-R)/a)}\,. \tag{2}$$

Here, $U = V_0\left(1-\beta\,\frac{N-Z}{A}\cdot t_z\right)$, $U_{ls} = V_{ls}\left(1-\beta_{ls}\,\frac{N-Z}{A}\cdot t_z\right)$, $R = r_0A^{1/3}$, t_z=1/2 for neutrons and $t_z = -1/2$ for protons. In the case of protons we added to (2) the potential of a uniformly charged sphere with $R_c = r_cA^{1/3}$. The parameters of potential used here were as follows: $V_0 = -51.0$ MeV, $V_{ls} = 32.4\,\mathrm{MeV\cdot fm^2}$, r_0=1.27 fm, r_c=1.25 fm, β=1.31, $\beta_{ls} = -0.6$, $a = 0.67$ fm for protons and $a = 0.55$ fm for neutrons. These parameters are very close to those from the paper [4].

The comparison of the empirical and theoretical (WS) values of the one-neutron separation energies S_p for the chains of isotones with $N = 50$ and $N = 51$ is shown in Fig. 4.

For description of excited states and transition rates we used the QRPA approach, see details in [2, 3], with the phenomenological mean field potential shown by us before, as well as the effective interaction, the same in the particle–particle, particle–hole, and pairing channels. This interaction was also used in our previous paper and has the form

$$\hat{\vartheta} = \Big(V + V_\sigma\sigma_1\sigma_2 + V_T S_{12} + V_\tau\tau_1\tau_2 + V_{\tau\sigma}\sigma_1\sigma_2\cdot\tau_1\tau_2 + V_{\tau T}S_{12}\tau_1\tau_2\Big)\exp\Big(-\frac{r_{12}^2}{r_{00}^2}\Big) + \frac{e^2}{r_{12}}\left(\frac{1}{2}-\hat{t}_z(1)\right)\left(\frac{1}{2}-\hat{t}_z(2)\right). \tag{3}$$

The entering parameters are as follows: $V = -16.65$, $V_\sigma = 2.33$, $V_T = -3.00$, $V_\tau = 3.35$, $V_{\tau\sigma} = 4.33$, $V_{\tau T} = 3.00$ (all these values are in MeV), while $r_{00} = 1.75$ fm.

Using the standard procedure we can pass to the quasiparticle basis, $a^+ \to \xi^+$:

$$a^+_\alpha = u_{|\alpha|}\xi^+_\alpha - v_{|\alpha|}\varphi_\alpha\xi_{-\alpha};\; u^2_{|\alpha|} + v^2_{|\alpha|} = 1;\; \varphi_\alpha = (-1)^{l_\alpha + j_\alpha - m_\alpha}. \tag{4}$$

We also define the creation operator $Q^+_{n,JM}$ of the one-phonon excited state $|\omega_n, JM\rangle$ with $|\omega_n, JM\rangle = Q^+_{n,JM}|\tilde{0}\rangle$ in the following way:

$$Q^+_{n,JM} = \sum_{a\geq b} X^{n,J}_{j_aj_b}\left[\xi^+_a\xi^+_b\right]_{JM} - \sum_{c\geq d} Y^{n,J}_{j_cj_d}\left[\xi_c\xi_d\right]_{JM}\,, \tag{5}$$

Then we obtain the set of the QRPA equations which define the amplitudes "X" and "Y" of the states $|\omega_n, JM\rangle$ and the eigenvalues ω_n, these equations have the form

$$\left\|\begin{matrix}[(E-\omega)I + A] & B \\ -B & -[(E+\omega)I + A]\end{matrix}\right\|\times\begin{pmatrix}X\\Y\end{pmatrix} = 0.. \tag{6}$$

Here, $E = E_{ab} = E_{j_a} + E_{j_b}$, $I_{cd,ab} = \delta_{j_aj_c}\delta_{j_bj_d}$, while the matrix elements of the sub-matrices A and B in the case of even–even nuclei are as follows [2, 3]:

$$\begin{aligned} A_{cd,ab} \equiv A^J_{j_cj_d,j_aj_b} &= \left(u_{j_c}u_{j_d}u_{j_a}u_{j_b} + v_{j_c}v_{j_d}v_{j_a}v_{j_b}\right)\times \\ &\times {}_a\langle j_cj_d;J|\hat{\vartheta}|j_aj_b;J\rangle_a + \\ &+ \left(u_{j_c}v_{j_d}u_{j_a}v_{j_b} + v_{j_c}u_{j_d}v_{j_a}u_{j_b}\right){}_a\langle j_c\bar{j}_d;J|\hat{\vartheta}|j_a\bar{j}_b;J\rangle_a + \\ &+ (-1)^{j_a+j_b+J+1}\left(v_{j_c}u_{j_d}u_{j_a}v_{j_b} + u_{j_c}v_{j_d}v_{j_a}u_{j_b}\right)\times \\ &\times {}_a\langle j_c\bar{j}_d;J|\hat{\vartheta}|j_b\bar{j}_a;J\rangle_a\,; \end{aligned} \tag{7}$$

$$\begin{aligned} B_{cd,ab} \equiv B^J_{j_cj_d,j_aj_b} &= \left(u_{j_c}u_{j_d}v_{j_a}v_{j_b} + v_{j_c}v_{j_d}u_{j_a}u_{j_b}\right)\times \\ &\times {}_a\langle j_cj_d;J|\hat{\vartheta}|j_aj_b;J\rangle_a - \left(u_{j_c}v_{j_d}v_{j_a}u_{j_b} + v_{j_c}u_{j_d}u_{j_a}v_{j_b}\right)\times \\ &\times {}_a\langle j_c\bar{j}_d;J|\hat{\vartheta}|j_a\bar{j}_b;J\rangle_a + (-1)^{j_a+j_b+J}\times \\ &\times \left(v_{j_c}u_{j_d}v_{j_a}u_{j_b} + u_{j_c}v_{j_d}u_{j_a}v_{j_b}\right){}_a\langle j_c\bar{j}_d;J|\hat{\vartheta}|j_b\bar{j}_a;J\rangle_a\,. \end{aligned} \tag{8}$$

In Eqs. (7) and (8), ${}_a\langle j_cj_d;J|\hat{\vartheta}|j_aj_b;J\rangle_a$ and ${}_a\langle j_c\bar{j}_d;J|\hat{\vartheta}|j_a\bar{j}_b;J\rangle_a$ are the antisymmetric matrix elements of the effective interaction $\hat{\vartheta}$ in the particle–particle and particle–hole channels with a given spin. They have the form

$$\begin{aligned} {}_a\langle j_cj_d;J|\hat{\vartheta}|j_aj_b;J\rangle_a &= \frac{1}{\sqrt{(1+\delta_{j_cj_d})(1+\delta_{j_aj_b})}}\times \\ &\times\Big[\langle j_cj_d;J|\hat{\vartheta}|j_aj_b;J\rangle + (-1)^{j_a+j_b+J+1}\langle j_cj_d;J|\hat{\vartheta}|j_bj_a;J\rangle\Big], \end{aligned} \tag{9}$$

$$\begin{aligned} {}_a\langle j_c\bar{j}_d;J|\hat{\vartheta}|j_a\bar{j}_b;J\rangle_a &= -\frac{(-1)^{l_b+l_d}}{\sqrt{(1+\delta_{j_cj_d})(1+\delta_{j_aj_b})}}\times \\ &\times\sum_{J'}(2J'+1)W[j_bj_aj_cj_d;JJ']\times \\ &\times\Big[\langle j_bj_c;J'|\hat{\vartheta}|j_dj_a;J'\rangle + (-1)^{j_d+j_a+J'+1}\langle j_bj_c;J'|\hat{\vartheta}|j_aj_d;J'\rangle\Big]. \end{aligned} \tag{10}$$

Using an explicit form of the matrix equation (6), we obtain the orthonormality relation

$$\left|\sum_{a\geq b}X^{n,J}_{j_aj_b}X^{m,J}_{j_aj_b} - \sum_{c\geq d}Y^{n,J}_{j_cj_d}Y^{m,J}_{j_cj_d}\right| = \delta_{mn}\,, \tag{11}$$

which in terms of the QRPA bosons corresponds to the condition

$$\langle\omega_n, JM|\,\omega_m, JM\rangle = \langle\tilde{0}|Q_{n,JM}\cdot Q^+_{m,JM}|\tilde{0}\rangle = \delta_{mn}\,. \tag{12}$$

The transition rate between the one-phonon and the ground state is described by the reduced matrix element, see also [2, 3]

$$\begin{aligned} \langle\tilde{0}||\mathcal{M}(\lambda)||\omega_n,J\rangle &= (-1)^\lambda\delta(J,\lambda)\delta(\pi_n\pi_\lambda)\times \\ &\times\Big[\sum_{j_a\geq j_b}X^{n,J}_{j_aj_b}(u_{j_a}v_{j_b}\pm v_{j_a}u_{j_b})\frac{(-1)^{l_b}}{\sqrt{1+\delta_{j_aj_b}}}\langle j_a||\hat{m}(\lambda)||j_b\rangle - \\ &- \sum_{j_a\geq j_b}Y^{n,J}_{j_aj_b}(v_{j_a}u_{j_b}\pm u_{j_a}v_{j_b})\frac{(-1)^{l_b}}{\sqrt{1+\delta_{j_aj_b}}}\langle j_a||\hat{m}(\lambda)||j_b\rangle\Big], \end{aligned} \tag{13}$$

Table 1. Root-mean-square radii of the proton and neutron distributions in $N = 50$ isotones. Empirical data are from [7, 8]

Z	$R_p(exp)$	$R_p(th)$	$R_n(th)$
27		3.933	4.196
28		3.957	4.198
29		3.989	4.208
30		4.019	4.218
31	4.044(9)	4.048	4.227
32		4.075	4.236
33		4.100	4.246
34		4.125	4.255
35		4.150	4.265
36	4.183(2)	4.174	4.274
37	4.199(2)	4.197	4.283
38	4.224(2)	4.219	4.292
39	4.243(2)	4.243	4.300
40	4.269(1)	4.267	4.308
41	4.288(4)	4.288	4.317
42	4.315(1)	4.310	4.325
43		4.331	4.333
44		4.351	4.341
45		4.372	4.349
46		4.391	4.357
47	4.420(23)	4.410	4.365
48		4.429	4.372
49		4.447	4.380
50		4.464	4.388
51		4.494	4.399

where the upper signs refer to T-even (Eλ), while the lower ones to T-odd (Mλ) transitions.

In Fig. 5, we show systematics of 2_1^+ levels and reduced transition rates $B(E2, 2_1^+ \rightarrow gr.st.)$ in even $N = 50$ isotones. One can see a good agreement with the experiment.

Table 1 shows the comparison of the empirical and theoretical (HF+BCS) root-mean-square radii for $N = 50$ isotones. The deviation from the experiment is no more than 0.2 %.

Figures 6–8 demonstrate proton and neutron densities for ^{78}Ni, ^{88}Sr, and ^{100}Sn calculated both in (HF+BCS) and (WS+BCS) approaches. Here, we see the characteristic behavior of densities by moving from neutron-excess to neutron-deficient nuclei. In particular, HF+BCS calculations, as compared to WS+BCS ones, give the more smooth variation of both proton and neutron densities as functions of radii.

Acknowledgements

This research was supported by the RSCF grant No 14-22-00281.

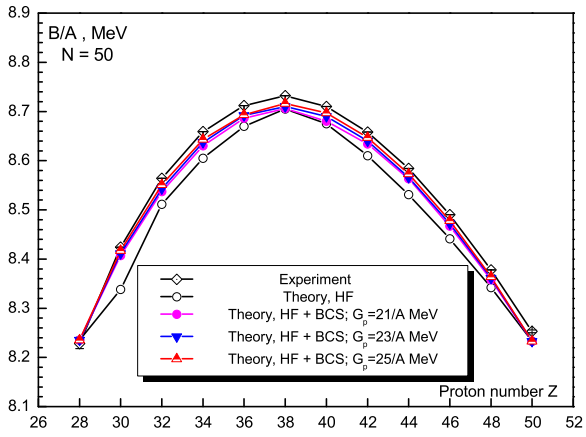

Figure 1. (Color online) Binding energies per nucleon, B/A in the chain of $N = 50$ isotones. All experimental data are from [6].

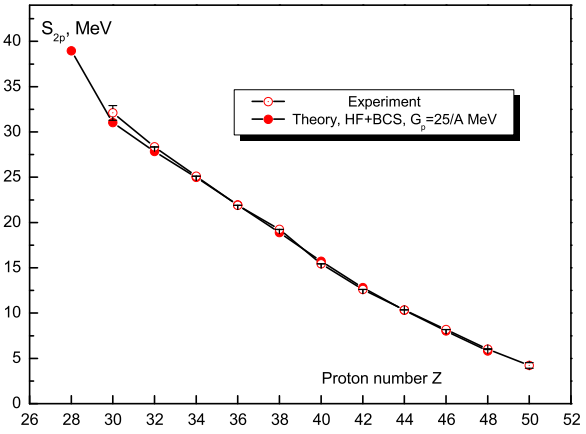

Figure 2. (Color online) Two-proton separation energies in the chain of $N = 50$ isotones. Empirical data are from [6].

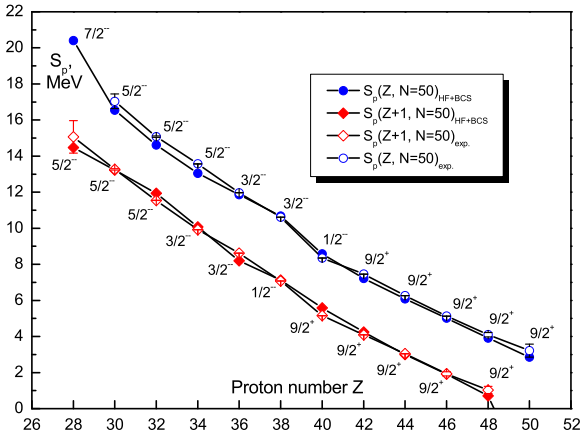

Figure 3. (Color online) Proton separation energies in the chain of $N = 50$ isotones, calculated in the HF+BCS scheme. Experimental data are from [6].

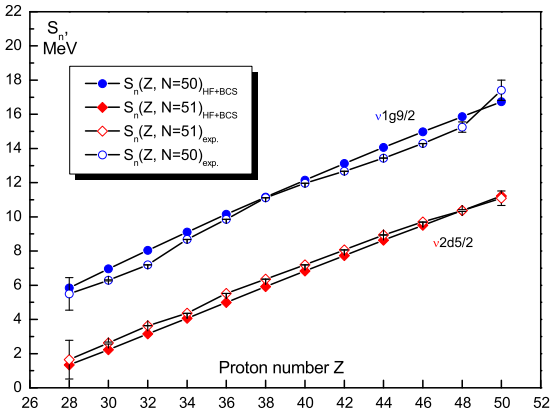

Figure 4. (Color online) Neutron separation energies for the chains of $N = 50$ and $N = 51$ isotones; WS scheme. The experimental data are from [6].

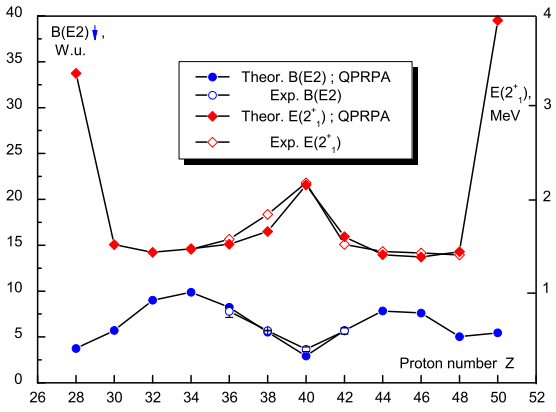

Figure 5. (Color online) Systematics of the energies of 2_1^+ levels and reduced transition rates, $B(E2; 2_1^+ \rightarrow gr.st.)$, in even $N = 50$ isotones. Here, $e_p(eff) = 1.3|e|$ and $e_n(eff) = 0.3|e|$. The experimental data are from [7].

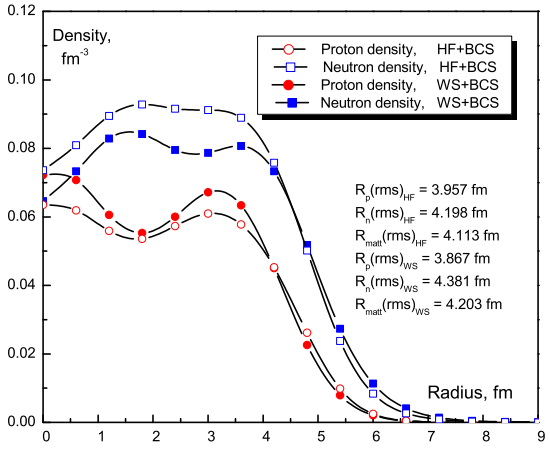

Figure 6. (Color online) Proton and neutron densities in ^{78}Ni.

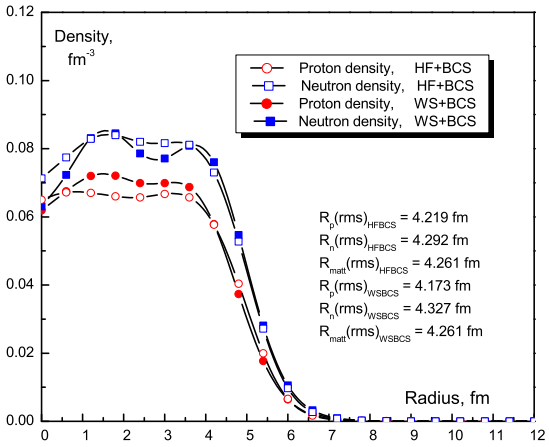

Figure 7. (Color online) Proton and neutron densities in ^{88}Sr.

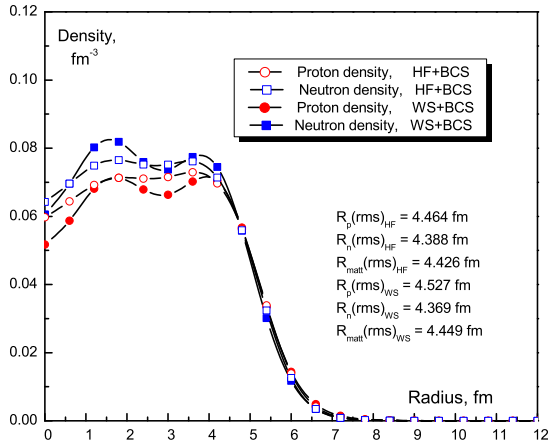

Figure 8. (Color online) Proton and neutron densities in ^{100}Sn.

References

[1] K.I. Erokhina, V.I. Isakov, B. Fogelberg, *et al.*, Part. and Nucl. Lett. No.4, **107**, 5 (2001)
[2] V.I. Isakov, Phys. At. Nucl. **73**, 1515 (2010)
[3] V.I. Isakov, Phys. At. Nucl. **76**, 828 (2013)
[4] V.I. Isakov, K.I. Erokhina, H. Mach, *et al.*, Eur. Phys. J. A **14**, 29 (2002)
[5] V.G. Soloviev, *Theory of Complex Nuclei* (Pergamon Press, Oxford, 1976)
[6] http://www-nds.iaea.org/amdc/
[7] http://www.nndc.bnl.gov/ensdf/
[8] I. Angeli and K.P. Marinova, At. Data Nucl. Data Tables, **99**, 69 (2013)